LOS PATH FOLLOWING FOR UNDERACTUATED UNDERWATER VEHICLE

Even Børhaug Kristin Y. Pettersen

Dept. of Engineering Cybernetics, Norwegian University of Science and Technology, NO-7491 Trondheim, Norway.
{Even.Borhaug,Kristin.Y.Pettersen}@itk.ntnu.no.

Abstract: In this paper, we propose a control scheme for path following of underactuated underwater vehicles. In particular, we propose a guidance law based on the the well-known principle of Line of Sight (LOS) guidance that is applicable to path following of any geometric path with known curvature and torsion. A conceptually simple guidance law is obtained by formulating the control problem in the Serret-Frenet coordinate frame. The guidance law generates desired trajectories for the orientation of the vehicle which is used as an input to an underlying tracking controller. A tracking controller is synthesized using integrator backstepping. The obtained results are illustrated with numerical simulations of the HUGIN AUV.

1. INTRODUCTION

In this paper we solve the problem of 3D *path following* for an underactuated underwater vehicle. In this context a path is a piecewise differentiable, time-independent curve in space. Given the path to be followed, the objective is to design a control system that force the underwater vehicle to converge to the desired path from any off-path initial location and to move along the path with desired forward speed. When solving a trajectory tracking problem, the path to be followed is parameterized in terms of time. That is, we specify the desired position of the vehicle along the path as a function of time, and design a control system to track the desired position. The path following problem, on the other hand, does not specify the desired position of the vehicle in terms of time and therefore does not put any constraints on the speed of the vehicle. This gives more operational flexibility, since the desired speed of the vehicle can be specified independently of the path.

Traditional control strategies for path following, such as *PID cross-track control* or *LOS cross-track control* are usually optimized for straight-line paths. Since such traditional control strategies are not designed to handle curved reference paths, the controller performance can be expected to degrade when the reference path is curved. Allowing curved reference paths gives the operators more flexibility at the planning stage and allows the underwater vehicle to perform more complex maneuvers with guaranteed performance, such as docking on stationary and moving underwater installations and performing seabed/contour following.

The available literature on 3D path following for *underactuated* underwater vehicles is sparse. (Encarnação *et al.*, 2000) presents a partial solution to the *planar* path following problem for underwater vehicles, and the results are extended to $3D$ path following in (Encarnação and Pascoal, 2000). However in both cases, the results are local and the initial position of the vehicle is restricted to lie inside a tube around the path, the radius of which must be smaller than the smallest radius of curvature that is present in the path. The relatively stringent condition on the initial position of the underwater vehicle is lifted in (Lapierre *et al.*, 2003) by introducing

the concept of a *virtual target*. By controlling the progression of the virtual target in a convenient manner, (Lapierre *et al.*, 2003) is able to solve the *planar* path following problem in the global sense. (Aicardi *et al.*, 2001) proposed a solution to the planar path following problem giving boundedness of the path error, but without requiring knowledge of the curvature. However, the obtained results are local and the proposed controller is not defined for zero path error.

In this paper, we propose a new control strategy for underwater vehicles expected to follow a general reference path in 3-dimensional space. We show that by formulating the path following problem in the *Serret-Frenet* coordinate frame and applying a LOS guidance law, the solution to the general path following problem is almost as easy as in the case of a straight-line reference paths. Moreover, we use the concept of current frame to allow the vehicle to move along the path with a non-zero angle of sideslip and a non-zero angle of attack. The proposed control strategy has a general nature, and can be easily adopted for path following of other mechanical systems.

2. DYNAMICAL MODEL

We consider an underactuated underwater vehicle described by the kinematic and dynamic model

$$\dot{\boldsymbol{\eta}} = \boldsymbol{J}(\boldsymbol{\eta})\boldsymbol{\nu}, \quad (1)$$

$$\boldsymbol{M}\dot{\boldsymbol{\nu}} + \boldsymbol{C}(\boldsymbol{\nu})\boldsymbol{\nu} + \boldsymbol{D}(\boldsymbol{\nu})\boldsymbol{\nu} + \boldsymbol{g}(\boldsymbol{\eta}) = \boldsymbol{B}_u\boldsymbol{u}, \quad (2)$$

where $\boldsymbol{\eta} \triangleq [x, y, z, \theta, \psi]^T$ and $\boldsymbol{\nu} \triangleq [u, v, w, q, r]^T$. Here, $\boldsymbol{p}^i \triangleq [x, y, z]^T$ is the 3-dimensional position of the underwater vehicle in inertial coordinates, $\boldsymbol{\Theta}_{ib} \triangleq [0, \theta, \psi]^T$ is the orientation of the body frame b with respect to the inertial frame i and $\boldsymbol{v}^b \triangleq [u, v, w]^T$ and $\boldsymbol{\omega}_{ib}^b \triangleq [0, q, r]^T$ are the body-fixed linear and the angular velocities respectively. The class of underwater vehicles considered in this paper is assumed to be passively stabilized in roll and we assume that the roll angle is limited. Hence, the roll mode is left out of the dynamical model used for control design purposes.

The matrix $\boldsymbol{M} = \boldsymbol{M}^T > 0$ is referred to as the mass and inertia matrix, $\boldsymbol{C}(\boldsymbol{\nu})$ the Coriolis and centripetal matrix and $\boldsymbol{D}(\boldsymbol{\nu})$ the damping matrix. Moreover, $\boldsymbol{g}(\boldsymbol{\eta})$ is a vector of restoring forces and moments due to gravity and buoyancy, and $\boldsymbol{B}_u$ is the control input matrix. The vector $\boldsymbol{u} = [T_u, \delta_S, \delta_D]^T$ is the control input where T_u is the surge thrust and δ_S and δ_D are steering and diving rudder deflections respectively. The matrix $\boldsymbol{B}_u$ is an actuator configuration matrix and is of full column rank.

3. SPACE CURVES AND THE SERRET-FRENET FORMULAS

For underwater vehicle operations, the desired path of the vehicle may be given as a space curve in a fixed inertial frame. Using the Serret-Frenet equations, the control problem can be formulated in the Serret-Frenet coordinate frame. We introduce the Serret-Frenet frame and equations in this section.

A space curve can be described entirely in terms of its *curvature* κ, *torsion* τ, and the initial starting point and direction. In particular, using the Serret-Frenet formulas (see e.g. (Frenet, 1847)), a space curve can be parameterized in terms of the arc length s according to:

$$\begin{bmatrix} \dot{\boldsymbol{T}} \\ \dot{\boldsymbol{N}} \\ \dot{\boldsymbol{B}} \end{bmatrix} = \dot{s} \begin{bmatrix} 0 & \kappa(s) & 0 \\ -\kappa(s) & 0 & \tau(s) \\ 0 & -\tau(s) & 0 \end{bmatrix} \begin{bmatrix} \boldsymbol{T} \\ \boldsymbol{N} \\ \boldsymbol{B} \end{bmatrix}, \quad (3)$$

where $\boldsymbol{T}$ is the unit tangent vector, $\boldsymbol{N}$ is the unit normal vector and $\boldsymbol{B}$ is the unit binormal vector (see Fig. 1).

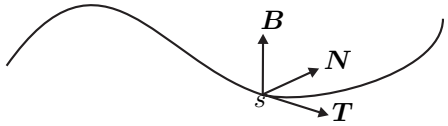

Fig. 1. The Serret-Frenet frame.

Note that the curvature and the torsion of a path is invariant with respect to reparameterization and is therefore an intrinsic property of the path. Physically, curvature may be conceived as the ratio of the normal acceleration of a particle, moving along the curve, to the particle's speed. This ratio measures the degree to which the curve deviates from the straight line at a particular point. The torsion of the curve measures the rate of roll relative to the particle's speed, that is the rate at which the osculating plane, i.e. the plane spanned by the vectors $\boldsymbol{T}$ and $\boldsymbol{N}$, rotates about the tangent vector $\boldsymbol{T}$.

The coordinate frame defined by the three unit vectors $\boldsymbol{T}$, $\boldsymbol{N}$ and $\boldsymbol{B}$ is referred to as the Serret-Frenet coordinate frame, and in this paper denoted the f-frame. Moreover, the linear velocity of the f-frame and angular velocity of the f-frame relative to the inertial frame i are given by (see e.g. (Egeland and Gravdahl, 2002)):

$$\boldsymbol{v}_f^f = \dot{s} \cdot \boldsymbol{T}, \quad (4)$$

$$\boldsymbol{\omega}_{if}^f = \dot{s} \cdot [\tau(s)\boldsymbol{T} + \kappa(s)\boldsymbol{B}]. \quad (5)$$

4. PROBLEM STATEMENT AND CONTROL OBJECTIVE

In this section, we use the Serret-Frenet formulas and Serret-Frenet coordinate frame description

introduced in the previous section and formulate the control problem in this frame.

We consider an underactuated underwater vehicle commanded to follow a given space curve, where the space curve is defined by its curvature $\kappa(s)$ and torsion $\tau(s)$. Moreover, the vehicle is commanded to follow a desired velocity profile $u_d(s)$ and we define the following surge speed control goal

$$\lim_{t\to+\infty} u(t) - u_d(s(t)) = 0. \tag{6}$$

Note that due to the underactuation of the vehicle it is important that the vehicle maintain a non-zero forward speed. This is necessary in order to make all state variables controllable. Therefore, we will assume that the desired speed profile is separated from zero and bounded, i.e. that there exists $U_{\min} > 0$ and $U_{\max} \geq U_{\min}$ such that $\forall s \in \mathbb{R}$,

$$0 < U_{\min} \leq u_d(s) \leq U_{\max} < \infty. \tag{7}$$

The dynamics of the underwater vehicle (2), is given in the body fixed coordinate frame b. Moreover, the orientation of the vehicle is defined as the orientation of the b-frame relative to the inertial frame i. However, when working with underactuated vehicles and arbitrary space curves it is often more natural to consider the orientation of the current frame c with respect to the i-frame. Next, we explain the meaning of current frame.

4.1 The Current Frame

The current frame c is a body fixed coordinate frame, with the origin located in the same point as the b-frame, but the orientation relative to the b-frame depends on the linear velocities of the vehicle. In particular, the c-frame is obtained by rotating the b-frame an angle α, where $\alpha \triangleq \tan^{-1}(w/u)$, about the b-frame y-axis and then an angle $-\beta$, where $\beta \triangleq \tan^{-1}(v/\sqrt{u^2+w^2})$, about the (rotated) z-axis. The angles α and β are commonly referred to as the angle of attack and angle of sideslip respectively.

Using the zyx convention for composite rotations, the rotation matrix from the b-frame to the c-frame is given by $\boldsymbol{R}_b^c \triangleq \boldsymbol{R}_z(-\beta)\boldsymbol{R}_y(\alpha)$. Furthermore, from the definition of α and β is follows that $\boldsymbol{U} \triangleq \boldsymbol{R}_b^c(\alpha,\beta)\boldsymbol{v}^b$, where $\boldsymbol{v}^b = [u,v,w]^T$, is all along the c-frame x-axis. That is, $\boldsymbol{U} = [U,0,0]^T$, where $U = \sqrt{u^2+v^2+w^2}$. The vector $\boldsymbol{U}$ and the scalar U are commonly referred to as the total velocity vector and the total speed respectively.

4.2 Path Following Control Goal

We consider a desired space curve $\boldsymbol{\Gamma}$ and place a Serret-Frenet frame f on the curve. We denote the position of the current frame c in the f-frame by

$$\boldsymbol{r}_{fc}^f \triangleq x_f\boldsymbol{T} + y_f\boldsymbol{N} + z_f\boldsymbol{B}, \tag{8}$$

where the parameter x_f can be seen as the along-track error and y_f and z_f as the the cross-track errors. Moreover, we denote the orientation of the c-frame relative to the f-frame by $\boldsymbol{\Theta}_{fc} \triangleq [\phi_{fc}, \theta_{fc}, \psi_{fc}]^T$. Note that even though we assume the roll angle of the vehicle to be zero, ϕ_{fc} is generally non-zero.

The linear velocity of the c-frame relative to the inertial frame i is given by

$$\boldsymbol{v}_c = \boldsymbol{v}_f + \frac{{}^i d}{dt}\boldsymbol{r}_{fc} = \boldsymbol{v}_f + \frac{{}^f d}{dt}\boldsymbol{r}_{fc} + \boldsymbol{\omega}_{if} \times \boldsymbol{r}_{fb}, \tag{9}$$

Decomposing the linear velocity in the f-frame and using the Serret-Frenet formulas (3) then gives

$$\boldsymbol{v}_c^f = \begin{bmatrix} \dot{s} + \dot{x}_f \\ \dot{y}_f \\ \dot{z}_f \end{bmatrix} + \dot{s}\begin{bmatrix} 0 & -\kappa & 0 \\ \kappa & 0 & -\tau \\ 0 & \tau & 0 \end{bmatrix}\begin{bmatrix} x_f \\ y_f \\ z_f \end{bmatrix}. \tag{10}$$

Note that a common approach is to choose the f-frame such that $x_f \equiv 0$, i.e. to locate the f-frame in the point on the path closest to the vehicle. However, as noted in (Lapierre *et al.*, 2003), this makes the computation of $\dot{s}$ from (10) singular for $y_f = 1/\kappa$. To avoid the singularity, we let x_f evolve according to a conveniently defined control law. That is, we add controlled dynamics to the origin of the f-frame in order to avoid the singularity in computing $\dot{s}$. In particular, we let x_f evolve according to

$$\dot{x}_f = -k_x x_f + \dot{s}\kappa y_f, \qquad k_x > 0. \tag{11}$$

Inserting (11) into (10) then gives

$$\boldsymbol{v}_c^f = \begin{bmatrix} \dot{s} \\ \dot{y}_f \\ \dot{z}_f \end{bmatrix} + \begin{bmatrix} -k_x & 0 & 0 \\ \dot{s}\kappa & 0 & -\dot{s}\tau \\ 0 & \dot{s}\tau & 0 \end{bmatrix}\begin{bmatrix} x_f \\ y_f \\ z_f \end{bmatrix}. \tag{12}$$

The first control goal was to achieve the desired velocity profile $u_d(s)$, see Eq. (6). The second control goal is to make the vehicle follow the desired space curve $\boldsymbol{\Gamma}$. Following definition (8), we must require that

$$\lim_{t\to+\infty} x_f(t) = y_f(t) = z_f(t) = 0. \tag{13}$$

Moreover, in order for the vehicle to move along the curve, we must make the total velocity vector $\boldsymbol{U}$ tangent to the curve. That is, the total velocity vector $\boldsymbol{U}$ must be aligned with the tangent vector $\boldsymbol{T}$. Equivalently, we must require that

$$\lim_{t\to+\infty} \theta_{fc}(t) = 0, \qquad \lim_{t\to+\infty} \psi_{fc}(t) = 0. \tag{14}$$

In particular, with $\theta_{fc} = \psi_{fc} = 0$ the c-frame x-axis is aligned with the f-frame x-axis and hence $\boldsymbol{U}$ is aligned with $\boldsymbol{T}$. Note that ϕ_{fc} does not affect the direction of the total velocity vector $\boldsymbol{U}$, and hence no control objective is required for ϕ_{fc}.

5. GUIDANCE LAW

In this section we propose a guidance law that gives desired trajectories for θ_{fc} and ψ_{fc}. The proposed guidance law is based on the Line of Sight (LOS) guidance principle.

We choose a point lying Δ meters ahead of the underwater vehicle, along the f-frame x-axis, and aim at it. We refer to the line joining the origin of the c-frame and the chosen point as the LOS line. Furthermore, the LOS line is characterized by the LOS angles

$$\theta_{\text{LOS}} = \tan^{-1}\left(\frac{z_f}{\sqrt{y_f^2 + \Delta^2}}\right), \tag{15}$$

$$\psi_{\text{LOS}} = -\tan^{-1}\left(\frac{y_f}{\Delta}\right), \tag{16}$$

giving the orientation of the LOS line with respect to the f-frame. See Figure 2 for a geometrical interpretation of the LOS angles. We propose using the LOS angles (15) and (16) as desired trajectories for θ_{fc} and ψ_{fc} respectively. Note that Δ must be strictly positive, but is not restricted to be constant. For instance, it might often be favorable to choose Δ as a function of s, κ or τ.

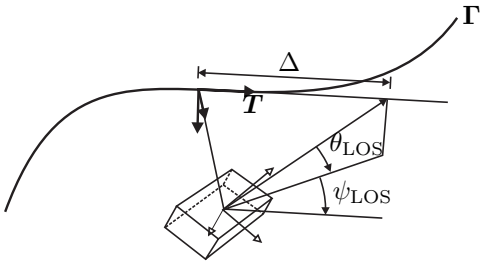

Fig. 2. LOS guidance in the Serret-Frenet frame.

Note that the curvature and torsion of the curve to be followed does not appear explicitly in the guidance laws (15)-(16). This is because the guidance laws gives the desired orientation of the c-frame with respect to the f-frame and not with respect to the inertial frame. The curvature and torsion of the path is captured by the Serret-Frenet coordinate frame description, making the guidance law appear as simple as in the case of straight-line paths, i.e. a path with $\kappa = \tau = 0$.

6. TRACKING CONTROLLER DESIGN

In this section, we propose a tracking controller for tracking the desired trajectories u_d, θ_{LOS} and ψ_{LOS}, where u_d satisfies (7) and θ_{LOS}, ψ_{LOS} are given by (15) and (16) respectively. The design is based on integrator backstepping.

We define the first tracking error as

$$\boldsymbol{z}_1 \triangleq \begin{bmatrix} \theta_{fc} \\ \psi_{fc} \end{bmatrix} - \begin{bmatrix} \theta_{\text{LOS}} \\ \psi_{\text{LOS}} \end{bmatrix}. \tag{17}$$

Differentiating $\boldsymbol{z}_1$ with respect to time and using the laws of differential kinematics (see e.g. (Egeland and Gravdahl, 2002)) gives

$$\dot{\boldsymbol{z}}_1 = \begin{bmatrix} \cos\phi_{fc} & -\sin\phi_{fc} \\ \dfrac{\sin\phi_{fc}}{\cos\theta_{fc}} & \dfrac{\cos\phi_{fc}}{\cos\theta_{fc}} \end{bmatrix} \boldsymbol{H}\boldsymbol{\omega}_{fc}^c - \begin{bmatrix} \dot{\theta}_{\text{LOS}} \\ \dot{\psi}_{\text{LOS}} \end{bmatrix}. \tag{18}$$

Here, $\boldsymbol{\omega}_{fc}^c$ denotes the angular velocity of the c-frame relative to the f-frame and $\boldsymbol{H}$ is a selection matrix defined as

$$\boldsymbol{H} \triangleq \begin{bmatrix} 0 & 1 & 0 \\ 0 & 0 & 1 \end{bmatrix}. \tag{19}$$

Furthermore, note that $\boldsymbol{\omega}_{fc}^c$ can be decomposed as

$$\boldsymbol{\omega}_{fc}^c = \boldsymbol{\omega}_{ic}^c - \boldsymbol{\omega}_{if}^c \tag{20}$$

$$= \boldsymbol{R}_b^c(\alpha,\beta)\boldsymbol{\omega}_{ib}^b + \boldsymbol{\omega}_{bc}^c - \boldsymbol{R}_f^c(\boldsymbol{\Theta}_{fc})\boldsymbol{\omega}_{if}^f, \tag{21}$$

where $\boldsymbol{\omega}_{ib}^b = [0, q, r]^T$, $\boldsymbol{\omega}_{bc}^c = [\dot{\beta}\sin\alpha, \dot{\alpha}, -\dot{\beta}\cos\alpha]^T$ and $\boldsymbol{\omega}_{if}^f$ is given by (5). Using (21), the error dynamics (18) can be written as

$$\dot{\boldsymbol{z}}_1 = \begin{bmatrix} \cos\phi_{fc} & -\sin\phi_{fc} \\ \dfrac{\sin\phi_{fc}}{\cos\theta_{fc}} & \dfrac{\cos\phi_{fc}}{\cos\theta_{fc}} \end{bmatrix} \cdot \left(\begin{bmatrix} \cos\beta & -\sin\beta\sin\alpha \\ 0 & \cos\alpha \end{bmatrix} \begin{bmatrix} q \\ r \end{bmatrix} - \boldsymbol{f}(t) \right). \tag{22}$$

Here, $\boldsymbol{f}(t)$ is a function defined as

$$\boldsymbol{f}(t) \triangleq \begin{bmatrix} \dot{\theta}_{\text{LOS}} \\ \dot{\psi}_{\text{LOS}} \end{bmatrix} - \boldsymbol{H}[\boldsymbol{\omega}_{bc}^c - \boldsymbol{R}_f^c(\boldsymbol{\Theta}_{fc})\boldsymbol{\omega}_{if}^f]. \tag{23}$$

Using the backstepping design methodology, we define a new error variable

$$\boldsymbol{z}_2 \triangleq \boldsymbol{\nu} - \boldsymbol{\chi} \tag{24}$$

where $\boldsymbol{\chi} \in \mathbb{R}^5$ is a vector of stabilizing functions to be determined. We want u to track u_d so we choose $\chi_1 = u_d$. Moreover, we use χ_4 and χ_5 as virtual controls to stabilize the $\boldsymbol{z}_1$-dynamics. In particular, we choose χ_4 and χ_5 according to

$$\begin{bmatrix} \chi_4 \\ \chi_5 \end{bmatrix} = -\begin{bmatrix} \cos\alpha & \sin\beta\sin\alpha \\ 0 & \cos\beta \end{bmatrix} \frac{1}{\cos\alpha\cos\beta} \cdot \left(\begin{bmatrix} \cos\phi_{fc} & \cos\theta_{fc}\sin\phi_{fc} \\ -\sin\phi_{fc} & \cos\theta_{fc}\cos\phi_{fc} \end{bmatrix} \boldsymbol{K}_1\boldsymbol{z}_1 - \boldsymbol{f}(t) \right), \tag{25}$$

where $\boldsymbol{K}_1 = \boldsymbol{K}_1^T > 0$. With this particular choice of χ_4 and χ_5, the $\boldsymbol{z}_1$-dynamics is given by

$$\dot{\boldsymbol{z}}_1 = -\boldsymbol{K}_1\boldsymbol{z}_1 + \boldsymbol{Q}(t)\boldsymbol{z}_2, \tag{26}$$

where $\boldsymbol{Q}(t)$ is defined as

$$\boldsymbol{Q}(t) \triangleq \begin{bmatrix} \cos\phi_{fc} & -\sin\phi_{fc} \\ \dfrac{\sin\phi_{fc}}{\cos\theta_{fc}} & \dfrac{\cos\phi_{fc}}{\cos\theta_{fc}} \end{bmatrix} \cdot \begin{bmatrix} \cos\beta & -\sin\beta\sin\alpha \\ 0 & \cos\alpha \end{bmatrix} \begin{bmatrix} \boldsymbol{0}_{2\times 2} & \boldsymbol{H} \end{bmatrix}. \tag{27}$$

For the next step of backstepping, we differentiate $\boldsymbol{z}_2$ with respect to time, multiply the result by $\boldsymbol{M}$ and use (2) to obtain

$$\boldsymbol{M}\dot{\boldsymbol{z}}_2 = -\left[\boldsymbol{C}(\boldsymbol{\nu}) + \boldsymbol{D}(\boldsymbol{\nu}) + \boldsymbol{g}(\boldsymbol{\eta})\right] + \boldsymbol{B}_u\boldsymbol{u} - \boldsymbol{M}\ddot{\boldsymbol{\chi}}.$$

Note that $\boldsymbol{u} \in \mathbb{R}^3$ and $\boldsymbol{z}_2 \in \mathbb{R}^5$, meaning that we have only three independent controls available to stabilize five degrees of freedom. However, we we can utilize the fact that χ_2 and χ_3 are undetermined.

Let $\boldsymbol{b}_i$ denote the i'th column of $\boldsymbol{B}_u$ and let $\boldsymbol{m}_i$ denote the i'th column of $\boldsymbol{M}$. Then,

$$\boldsymbol{B}_u\boldsymbol{u} - \boldsymbol{M}\ddot{\boldsymbol{\chi}} = \boldsymbol{\Pi}_1 \begin{bmatrix} \boldsymbol{u} \\ \dot{\chi}_2 \\ \dot{\chi}_3 \end{bmatrix} - \boldsymbol{\Pi}_2 \begin{bmatrix} \dot{\chi}_1 \\ \dot{\chi}_5 \\ \dot{\chi}_6 \end{bmatrix}, \quad (28)$$

where $\boldsymbol{\Pi}_1 \triangleq [\boldsymbol{b}_1\ \boldsymbol{b}_2\ \boldsymbol{b}_3\ -\boldsymbol{m}_2\ -\boldsymbol{m}_3]$ and $\boldsymbol{\Pi}_2 \triangleq [\boldsymbol{m}_1\ \boldsymbol{m}_5\ \boldsymbol{m}_6]$. Now, if $\boldsymbol{\Pi}_1$ is non-singular, we can take

$$\begin{bmatrix} \boldsymbol{u} \\ \dot{\chi}_2 \\ \dot{\chi}_3 \end{bmatrix} = \boldsymbol{\Pi}_1^{-1}(\boldsymbol{\Pi}_2 \begin{bmatrix} \dot{\chi}_1 \\ \dot{\chi}_5 \\ \dot{\chi}_6 \end{bmatrix} + \boldsymbol{C}(\boldsymbol{\nu})\boldsymbol{\nu} + \boldsymbol{D}(\boldsymbol{\nu})\boldsymbol{\nu} + \boldsymbol{g}(\boldsymbol{\eta}) - \boldsymbol{K}_2\boldsymbol{z}_2 - \boldsymbol{Q}^T(t)\boldsymbol{z}_1), \quad (29)$$

where $\boldsymbol{K}_2 = \boldsymbol{K}_2^T$. The resulting closed loop error dynamics is then

$$\begin{bmatrix} \dot{\boldsymbol{z}}_1 \\ \boldsymbol{M}\dot{\boldsymbol{z}}_2 \end{bmatrix} = \begin{bmatrix} -\boldsymbol{K}_1 & \boldsymbol{Q}(t) \\ -\boldsymbol{Q}^T(t) & -\boldsymbol{K}_2 \end{bmatrix} \begin{bmatrix} \boldsymbol{z}_1 \\ \boldsymbol{z}_2 \end{bmatrix}. \quad (30)$$

Using the Lyapunov function $V = 1/2\boldsymbol{z}_1^T\boldsymbol{z}_1 + 1/2\boldsymbol{z}_2^T\boldsymbol{M}\boldsymbol{z}_2$ it is straightforward to verify that the origin $(\boldsymbol{z}_1, \boldsymbol{z}_2) = (\boldsymbol{0}, \boldsymbol{0})$ is exponentially stable. In particular, this implies that $u \to u_d$, $\theta_{fc} \to \theta_{\text{LOS}}$ and $\psi_{fc} \to \theta_{\text{LOS}}$ exponentially.

Remark: The above stability conclusion is not valid for $\alpha = \pm\pi/2$ or $\beta = \pm\pi/2$. These conditions occur if $\{u = 0, w \neq 0\}$ or $\{u = w = 0, v \neq 0\}$. In either case equation (25) is singular and χ_4 and χ_5 cannot be determined. This is however not a problem, since the vehicle must be moving forward for all the states to be controllable. Also, the rudders have no effect when $u = 0$. Thus in practice, the vehicle should start moving forward before the tracking controller is switched on. Note also that the desired surge speed profile is bounded from below by $U_{\min} > 0$, see Eq. (7), such that after transients $u(t) \geq U_{\min}$ for all future time and hence $\alpha, \beta \in (-\pi/2, \pi/2)$.

7. STABILITY TO THE DESIRED PATH

In the previous section, we proposed a tracking controller that guaranteed tracking of the desired surge speed profile u_d, and hence achievement of the control goal (6), together with tracking of the LOS angles (15)-(16). In this section, we show that achievement of the control goal (6) and tracking of the LOS angles also guarantees achievement of the remaining control goals (13) and (14).

The path following errors are the along-track error x_f and the cross-track errors y_f and z_f. The path following error dynamics is obtained from (11) and (12):

$$\dot{x}_f = -k_x x_f + \dot{s}\kappa y_f \quad (31a)$$
$$\dot{y}_f = U\sin\psi_{fc}\cos\theta_{fc} - \dot{s}\kappa x_f + \dot{s}\tau z_f \quad (31b)$$
$$\dot{z}_f = -U\sin\theta_{fc} - \dot{s}\tau y_f. \quad (31c)$$

From the previous section, we know that $u \to u_d$, $\theta_{fc} \to \theta_{\text{LOS}}$ and $\psi_{fc} \to \psi_{\text{LOS}}$ exponentially under closed loop control. Moreover, on the manifold $\{u = u_d, \theta_{fc} = \theta_{\text{LOS}}, \psi_{fc} = \psi_{\text{LOS}}\}$, we have the resulting path following error dynamics

$$\dot{x}_f = -k_x x_f + \dot{s}\kappa y_f \quad (32a)$$
$$\dot{y}_f = U_d\sin\psi_{\text{LOS}}\cos\theta_{\text{LOS}} - \dot{s}\kappa x_f + \dot{s}\tau z_f \quad (32b)$$
$$\dot{z}_f = -U_d\sin\theta_{\text{LOS}} - \dot{s}\tau y_f, \quad (32c)$$

where $U_d \triangleq \sqrt{u_d^2 + v^2 + w^2} \geq U_{\min} > 0$. Inserting (15) and (16) for θ_{LOS} and ψ_{LOS} respectively, then gives

$$\begin{bmatrix} \dot{x}_f \\ \dot{y}_f \\ \dot{z}_f \end{bmatrix} = \begin{bmatrix} -k_x x_f \\ -\dfrac{U_d y_f}{\sqrt{y_f^2 + z_f^2 + \Delta^2}} \\ -\dfrac{U_d z_f}{\sqrt{y_f^2 + z_f^2 + \Delta^2}} \end{bmatrix} + \dot{s} \begin{bmatrix} 0 & -\kappa & 0 \\ \kappa & 0 & \tau \\ 0 & -\tau & 0 \end{bmatrix} \begin{bmatrix} x_f \\ y_f \\ z_f \end{bmatrix}. \quad (33)$$

Note that the last term in (33) has a skew-symmetric structure and will not affect the stability of the system. In particular, it can be verified that the system (33) is uniformly globally asymptotically stable (UGAS) using the quadratic Lyapunov function $V = 1/2x_f^2 + 1/2y_f^2 + 1/2z_f^2$. Note that UGAS of the system (33) implies achievement of the control goal (13). Moreover, as $\{x_f, y_f, z_f\} \to 0$ it follows from (15) and (16) that $\theta_{\text{LOS}} \to 0$ and $\psi_{\text{LOS}} \to 0$. Then, since $\theta_{fc} \to \theta_{\text{LOS}}$ and $\psi_{fc} \to \psi_{\text{LOS}}$ exponentially under closed loop control, this also guarantees achievement of the control goal (14).

Remark: Above we analyzed the resulting path following dynamics on the manifold $\{u = u_d, \theta_{fc} = \theta_{\text{LOS}}, \psi_{fc} = \psi_{\text{LOS}}\}$, i.e. system (32). This was motivated by the fact that the tracking controller (29) guarantees exponential convergence of the controller errors to the manifold. To prove that the path following errors remain bounded while the controller errors are converging, one can use results from nonlinear cascaded systems theory, see e.g. (Panteley and Loria, 1998). This was done for example in (Børhaug *et al.*, 2006) for a similar system. See the reference for details.

8. SIMULATIONS

The proposed control system for path following was simulated with the HUGIN AUV following a circular helix with radius 20 meters and a vertical separation of 6π meters. The curvature and torsion of this helix is

$$\kappa = \frac{20}{20^2 + 3^2} = \frac{20}{409}, \quad \tau = \frac{3}{20^2 + 3^2} = \frac{3}{409}.$$

The underwater vehicle was given an initial horizontal path error of 10 meters and a vertical path error of 5 meters. The initial surge speed of the vehicle was 1.0 m/s and the desired surge speed was 1.5 m/s. Both rudders were saturated at $\pm 20^\circ$ and $\pm 10^\circ/s$. The look-ahead distance was chosen as $\Delta = 25$ [m] and the controller gains were chosen as $\boldsymbol{K}_1 = \text{diag}(35, 35)$ and $\boldsymbol{K}_2 = \text{diag}(50, 100, 100, 50, 50)$. For the model of HUGIN, the matrix $\boldsymbol{\Pi}_1$ is nonsingular and $|\det \Pi_1| = 1.4753 \cdot 10^{12}$. Simulation results are shown in Figure 3.

9. CONCLUSIONS

In this paper, we have proposed a new control strategy for 3D path following of underactuated underwater vehicles. In particular, we formulated the control problem in the Serret-Frenet coordinate frame and proposed a guidance law based on the Line of Sight (LOS) guidance principle. Then, we designed a nonlinear tracking control law for tracking the orientation given by the LOS guidance system and proved stability of the vehicle to the desired path. The obtained results were illustrated with numerical simulations of the HUGIN AUV.

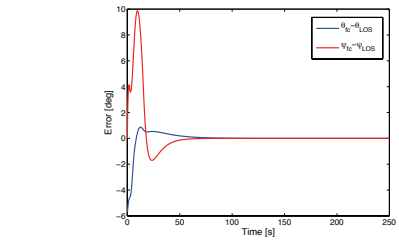

(a) Orientation errors.

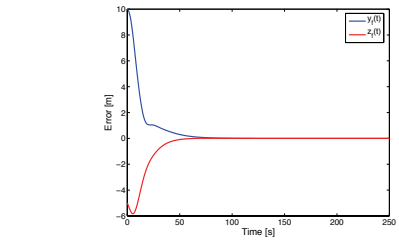

(b) Path errors $y_f(t)$ and $z_f(t)$.

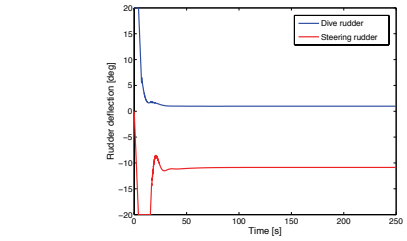

(c) Rudder deflections.

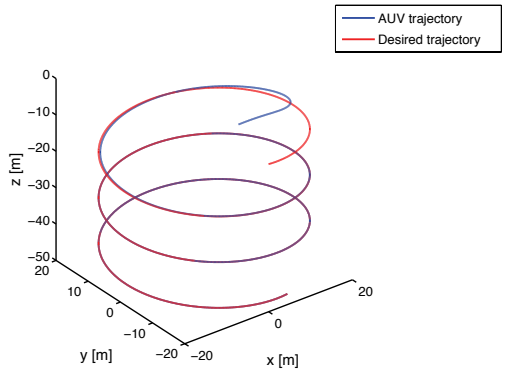

(d) xyz-trajectory.

Fig. 3. HUGIN AUV following circular helix.

REFERENCES

Aicardi, M., G. Casalino, G. Indiveri, A. Aguiar, P. Encarnação and A.M. Pascoal (2001). A planar path following controller for underactuated marine vehicles. In: *Proc. of 9th IEEE Mediterranean Conference on Control and Automation*. Dubrovnik, Croatia.

Børhaug, E., A. Pavlov and K. Y. Pettersen (2006). Cross-track formation control of underactuated autonomous underwater vehicles. In: *Group Coordination and Cooperative Control* (K. Y. Pettersen, J. T. Gravdahl and H. Nijmeijer, Eds.). Vol. 336. Springer Verlag.

Egeland, O. and J.T. Gravdahl (2002). *Modeling and Simulation for Automatic Control*. Marine Cybernetics. Trondheim, Norway.

Encarnação, P., A.M. Pascoal and M. Arcak (2000). Path following for autonomous marine craft. In: *Proc. of 5th IFAC Conference on Maneuvering and Control Marine Craft*. pp. 117–122.

Encarnação, P. and A.M. Pascoal (2000). 3D path following for autonomous underwater vehicle. In: *Proc. 39th IEEE Conference on Decision and Control*. Sydney, Australia. pp. 2977–2982.

Frenet, F. (1847). Sur les courbes à double courbure. PhD thesis. Toulouse, France.

Lapierre, L., D. Soetanto and A. Pascoal (2003). Nonlinear path following with applications to the control of autonomous underwater vehicles. In: *Proc. of the 42st IEEE Conference on Decision and Control*. Hawaii, USA. pp. 1256–1261.

Panteley, E. and A. Loria (1998). On global uniform asymptotic stability of nonlinear time-varying system in cascade. *System and Control Letters* **33**, 131–138.